Quanta Image Sensor Jot With Sub 0.3e- r.m.s. Read Noise and Photon Counting Capability

Jiaju Ma, *Student Member, IEEE*, and Eric R. Fossum, *Fellow, IEEE*

***Abstract*— The first quanta image sensor jot with photon counting capability is demonstrated. The low-voltage device demonstrates less than 0.3e- r.m.s. read noise on a single read out without the use of avalanche gain and single-electron signal quantization is observed. A new method for determining read noise and conversion gain is also introduced.**

***Index Terms*— CMOS image sensor, quanta image sensor, jot device, photon counting, high conversion gain, low read noise.**

I. Introduction

FOR the first time, an image sensor sense node is reported that has sufficiently low capacitance that a single electron's direct effect on the node voltage is clearly visible above background noise with a single correlated-double-sampling (CDS) read-out at room temperature, thus enabling photon (or photoelectron) counting without the use of avalanche gain. Such a capability will enable a new generation of high resolution image sensors for studying life-science phenomena, operation in ultra-low light conditions, and possible use in quantum encryption, among other applications.

The Quanta Image Sensor (QIS) has been proposed as a specialized CMOS image sensor in which each pixel has sufficient sensitivity to count photoelectrons, either as a single-bit QIS or multi-bit QIS [1], [2]. Each specialized pixel in a QIS is called a "jot" where multiple jots are needed to create an image pixel. The single-bit QIS needs a full-well capacity (FWC) of at least one electron, and multi-bit jots require a FWC of at most a few hundred electrons.

A single-photon avalanche diode (SPAD), 8μm pitch "jot" array has been used as a QIS image sensor and showed interesting results [3], [4]. SPADs, while excellent for photon timing applications, inherently require avalanche, resulting in high internal electric fields and high dark count rates that limit pitch and manufacturing yield. Thus, they are not expected to scale well to the sub-micron pitch and multi-megajot resolution needed for anticipated QIS applications. Avoiding avalanche-mode operation is a goal in the image sensor field.

Recently, a non-avalanche, low voltage "pump-gate" jot was proposed [5], [6] to achieve very low sense node capacitance and high conversion gain (CG). The pump-gate (PG) jot and a pump-gate jot with tapered reset gate (tapered PG) were both simulated in TCAD showing CG of 250μV/e- and 380μV/e- respectively. The devices use intra-pixel charge transfer from a vertically integrated storage site to a distal floating diffusion (FD). Implemented in a 65nm backside-illumination (BSI) commercial CMOS image sensor process, known to have high fill factor and quantum efficiency, with some implant and mask changes (but no additional masks), the pixels readily achieved 1.4μm pixel pitch for non-shared readout, and 1.0μm pitch for shared readout layout. Additional shrink of size in the same process is possible in the future. Layout of the jots was shown in [6].

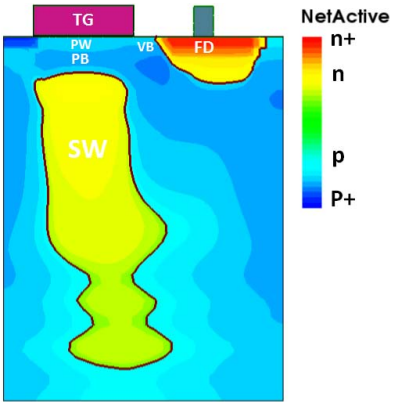

Fig. 1. The TCAD simulation cross-section doping profile of a pump gate jot device.

According to one theoretical model [7], to achieve photo-electron counting, a jot device needs an input-referred read noise level as low as 0.3e- r.m.s., though the model of [2] suggests that read noise less than 0.15e- r.m.s. is ultimately desired. In this letter, the first jot device with sub-0.3e- r.m.s. read noise is demonstrated and signal quantization observed.

II. Pump-Gate Jot Device Design and Operation

The simulated doping profile of a jot device with a pump-gate type charge transfer gate is depicted in Fig. 1. With a distal floating diffusion bridged to the transfer gate (TG) by a virtual barrier (VB) region, the FD has no overlap with TG, and with the pump-gate doping profile, the charge in the storage well (SW) will be transferred to the PW region underneath the TG when TG is pulsed "on", and then be laterally pumped over the VB region to the FD when TG turns "off". With small FWC in the SW, complete charge transfer can be achieved. Using this technique, the overlap capacitance between TG and FD can be eliminated.

Manuscript received June 13, 2015; revised July 9, 2015; accepted July 11, 2015. Date of publication July 13, 2015; date of current version August 21, 2015. This work was supported by Rambus, Inc., Sunnyvale, CA, USA. The review of this letter was arranged by Editor J.-M. Liu.

The authors are with the Thayer School of Engineering at Dartmouth, Hanover, NH 03755 USA (e-mail: eric.r.fossum@dartmouth.edu).

Color versions of one or more of the figures in this letter are available online at http://ieeexplore.ieee.org.

Digital Object Identifier 10.1109/LED.2015.2456067

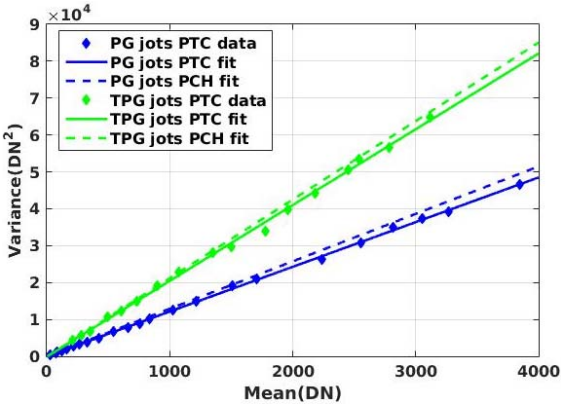

Fig. 2. Photon transfer curve (PTC) of jot devices with best fit lines (solid). Also shown are lines (dashed) corresponding to PCH results.

To further reduce the FD capacitance a tapered gate reset transistor [8] was employed. It uses a tapered shallow trench isolation (STI) to reduce the width of the channel of the reset transistor on the FD side so that the overlap capacitance between the reset gate (RG) and the FD can be reduced.

Both devices were taped out to the TSMC 65nm BSI process. Implantation conditions were modified according to simulation and the requirements of the jot devices.

The fabricated chip contains twenty 32×32 jots arrays with different mask variations. Each array connects to an on-chip switched-capacitor programmable gain amplifier (PGA) with designed gains of 8, 16 and 24. The PGAs output the analog signal to a pad through a single source-follower buffer. In this letter, two of the twenty variations are reported.

III. Testing Results

A. Photon Transfer Curve

For noise measurement, the chip was tested with an off-chip 14-bit ADC yielding over 10DN/e-, jot-referred. Correlated double-sampling and subsequent noise measurements are performed within the digital domain. The conversion gain of the two types of jots were obtained using the well-known photon transfer curve (PTC) method. The jots in a 32×32 array were selected and read out in sequence for multiple frames, and the variance of each jot's signal with different light intensity was measured. As shown in Fig. 2, the PTC of the PG jot array has a mean slope of 12.1 DN (19.9μV/DN), yielding a CG of 242μV/e- after the in-jot source-follower, which matches the result obtained with TCAD. The measured FWC is 288e-. The same method was used to test a 32×32 array of tapered PG jots. The PTC has a mean slope of 20.1 DN (20.0μV/DN) that yields a CG of 403μV/e-. The testing also shows the tapered PG jots have smaller FWC of 210e- compared to the PG jots.

B. Read Noise and Dark Signal

The read noise of both types of jots was measured in the dark with an integration time less than 5μsec and a CDS period of 20μsec. The measured total output-referred read noise of the PG jots is 96.9μVr.m.s., or 0.40e- r.m.s., input referred. The total output-referred read noise of the tapered PG jots is 136.9μVr.m.s., or 0.34e- r.m.s., input referred. The PG jots may have a lower voltage read noise because they have bigger source-follower gate area, so that lower 1/f noise is expected [9]. Room temperature dark signal was observed to be less than 1e-/s in the measured devices.

C. Photoelectron Counting Histogram

For the photoelectron counting histogram (PCH), jots are readout multiple times under fixed light level, and a histogram of signal levels is made. According to the theoretical model in [2], if the read noise is zero, the histogram should ideally consist of a series of narrow "spikes" corresponding to integer photoelectron numbers with amplitudes determined by the Poisson distribution. But, due to read noise, these spikes broaden and overlap. For read noise greater than approximately 0.5e- r.m.s., the peaks are so broad that no modulation in the histogram can be discerned and the quantized response is fully blurred by read noise. As was depicted in [2], for read noise below 0.5e- r.m.s., peaks and valleys emerge in the histogram and are fully formed when the read noise drops below 0.15e- r.m.s.. We term this condition where peaks and valleys are discernible, the deep sub-electron read noise regime.

Using the expressions derived in [2], it is possible to plot the valley-to-peak modulation (VPM) for the highest peak P_p and its highest adjacent valley P_v as a function of read noise, where VPM $= 1 - P_v/P_p$. The results are shown in Fig. 3 along with an approximate analytical expression for VPM. The accuracy of photoelectron counting increases as the modulation approaches unity due to reduction in bit error rate. By experimentally measuring the valley-to-peak modulation, one can use Fig. 3 to deduce read noise. VPM is a new method for determining read noise suitable for QIS devices and can readily allow noise measurements with sub-electron accuracy independent of CG determination. By measuring the distance between peaks, the CG can be measured since the peak separation should be one electron. This can be a new method to measure the CG in jot devices.

The PCH-VPM method was used to characterize the devices. A single jot was selected and read out 200,000 times under fixed light intensity and integration time. The histogram of the signals from a pump-gate jot is depicted in Fig. 4. The histogram clearly shows a quantization effect. Peaks are evenly separated (33.0DN at 7.7μV/DN), yielding a CG of 256μV/e-, which is 6% higher than the result from the PTC. The relative heights of peaks corresponds to the Poisson distribution with an average signal of ~6.5e-. VPM indicates a read noise of 0.32e- r.m.s. which is 0.08e- r.m.s. lower than obtained from the dark measurement.

The histogram of the tapered PG jot shows a stronger quantization effect. As shown in Fig. 5, the average signal level is ~5.2e-, and the distance between peaks is 59.3DN at 7.2μV/DN, and the CG of 426μV/e- is 6% higher than the PTC result. VPM yields a read noise 0.28e- r.m.s., 0.06e- r.m.s. lower than obtained from the dark measurement. The ADC input-referred calibration (μV/DN) in the PCH mea-

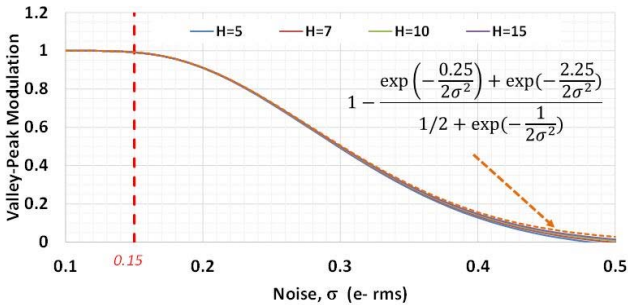

Fig. 3. Valley-to-peak modulation as a function of read noise for different histogram mean values H (e-). Read noise of less than 0.15e- r.m.s. is desired. For read noise above 0.5e- r.m.s., peaks become indistinct.

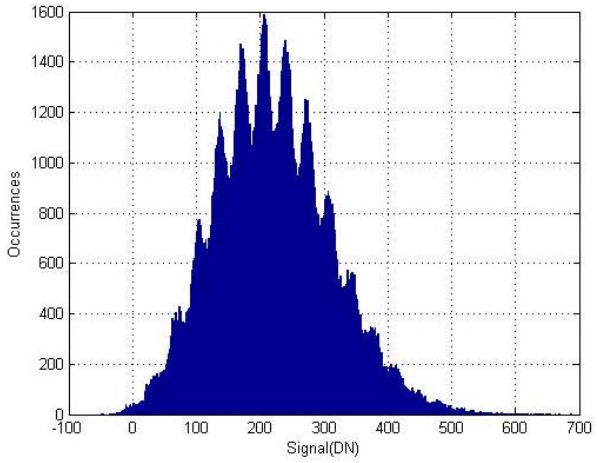

Fig. 4. Histogram of 200,000 reads of PG jot with average signal level of ∼6.5e- and 33DN/e-.

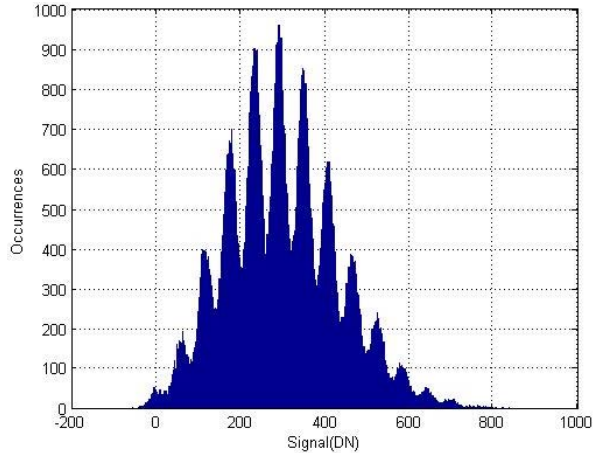

Fig. 5. Histogram of 200,000 reads of tapered PG jot with average signal level of ∼5.2e- and 59DN/e-.

surements is different from the PTC measurements because a higher PGA gain is used in the PCH method.

Measurements are summarized in Table 1. We believe that PCH and VPM methods yield a more accurate measurement of CG and read noise in this low-light regime since they are made directly under actual imaging operation, without artificial timing and with fewer sources of error. They also relate to what we care about most, photon counting capability.

TABLE I
JOT CHARACTERISTICS

	PG jot	Tapered PG jot
Pitch Size	1.4μm	1.4μm
Col. Bias Current	416nA	416nA
PTC CG	242 μV/e-	403 μV/e-
Dark Read Noise	97 μV r. m. s.	137 μV r. m. s.
PTC Read Noise	0.40e- r.m.s.	0.34e- r.m.s.
PCH CG	256 μV/e-	426 μV/e-
VPM Read Noise	0.32e- r.m.s.	0.28e- r.m.s.
Full Well Capacity	288e-	210e-
RT Dark Current	<1e-/s	<1e-/s

PTC measures CG using a broad range of signal (hundreds or thousands of electrons), whereas PCH measures CG with a signal of a few electrons. Thus, the voltage-dependent FD capacitance can reduce the measured CG when using PTC. In Fig. 2, straight lines using PCH measurement can be used to visually compare the results of the two methods. Note that the PCH measurement corresponds to very low values of DN in Fig. 2.

IV. CONCLUSION

In this letter, the testing results of a jot fabricated with a 65nm BSI CIS process is reported. The results show that the tested jot device has read noise as low as 0.28e- r.m.s., and a strong quantization effect was observed. For the first time, photoelectron counting is proven to be feasible in CMOS image sensors without avalanche gain, enabling a new generation of highly sensitive, high resolution image sensors.

ACKNOWLEDGMENTS

The authors appreciate discussions with M. Guidash, the fabrication work done by TSMC, and the technical assistance of A. Rao and other members of our group at Dartmouth.

REFERENCES

[1] E. R. Fossum, "What to do with sub-diffraction-limit (SDL) pixels?—A proposal for a gigapixel digital film sensor (DFS)," in *Proc. IEEE Workshop CCDs Adv. Image Sensors*, Sep. 2005, pp. 214–217.

[2] E. R. Fossum, "Modeling the performance of single-bit and multi-bit quanta image sensors," *IEEE J. Electron Devices Soc.*, vol. 1, no. 9, pp. 166–174, Sep. 2013.

[3] N. A. W. Dutton *et. al*, "320×240 oversampled digital single photon counting image sensor," in *Symp. VLSI Technol. Dig. Tech. Papers*, Jun. 2014, pp. 1–2.

[4] N. A. W. Dutton *et. al*, "Oversampled ITOF imaging techniques using SPAD-based quanta image sensors," in *Proc. Int. Image Sensor Workshop (IISW)*, Jun. 2015, pp. 170–173.

[5] J. Ma, D. B. Hondongwa, and E. R. Fossum, "Jot devices and the quanta image sensor," in *Proc. Int. Electron Devices Meeting (IEDM)*, Dec. 2014, pp. 247–250.

[6] J. Ma and E. R. Fossum, "A pump-gate jot device with high conversion gain for a quanta image sensor," *IEEE J. Electron Devices Soc.*, vol. 3, no. 2, pp. 73–77, Mar. 2015.

[7] N. Teranishi, "Required conditions for photon-counting image sensors," *IEEE Trans. Electron Devices*, vol. 59, no. 8, pp. 2199–2205, Aug. 2012.

[8] M. Guidash, private communication, Apr. 2014.

[9] C. T. Rogers and R. A. Buhrman, "Composition of $1/f$ noise in metal-insulator-metal tunnel junctions," *Phys. Rev. Lett.*, vol. 53, no. 13, pp. 1272–1275, Sep. 1984.